Acta Cryst. (1998). B**54**, 766–773

New Measure of Distortion for Coordination Polyhedra

EMIL MAKOVICKY* AND TONČI BALIĆ-ŽUNIĆ

Geological Institute, University of Copenhagen, Øster Voldgade 10, DK-1350 København K, Denmark. E-mail: emilm@geo.geol.ku.dk

(*Received 16 October 1997; accepted 6 March 1998*)

Abstract

A new global measure of distortion for coordination polyhedra is proposed, based on a comparison of the ratios V_s(circumscribed sphere)/V_p(polyhedron) calculated, respectively, for the real and ideal polyhedra of the same number of coordinated atoms which have the same circumscribed sphere. This formula can be simplified to $\upsilon\,(\%) = 100[V_i(\text{ideal}) - V_r(\text{real})]/V_i$, where V_i and V_r are the volumes of the above-defined polyhedra. The global distortion can be combined with other polyhedral characteristics, *e.g.* with the eccentricity of the central atom in the polyhedron or with the degree of sphericity of the coordination sphere [Balić Žunić & Makovicky (1996). *Acta Cryst.* B**52**, 78–81]. V_s/V_p ratios are given for a number of ideal polyhedra, including several types of trigonal coordination prisms, with the aim of facilitating the distortion calculations. The application examples included in the paper are: complex sulfides based on PbS and SnS archetypes, coordination polyhedra of large cations in feldspars, a phase transformation in a monoclinic amphibole and the subdivision of structures isopointal to ilmenite.

1. Introduction

Coordination polyhedra of ligand atoms around a central atom are one of the fundamental notions of crystal chemistry. Although the concept is straightforward, its application to real structures is fraught with practical problems connected with the departures of the coordination polyhedra from regularity.

The number of coordinated atoms (CN) is obvious for regular/ideal coordination polyhedra; a number of weighting schemes or cut-off procedures were devised for dealing with more distant ligands in deformed polyhedra (*e.g.* Carter, 1978).

Whenever possible, the shape of a polyhedron is compared with that of an ideal or regular one (*e.g.* Lueken *et al.*, 1987). Departures from ideality are mostly treated in the literature by procedures specific for a given polyhedron and problem [*e.g.* mean quadratic elongation (Robinson *et al.*, 1971), measures of octahedral flattening and deformation in phyllosilicates (Toraya, 1981; Weiss *et al.*, 1985) and symmetry-deformation coordinates (Klebe & Weber, 1994)].

It is impossible to devise a completely model-free measure of polyhedral distortion. Ideal polyhedra and coordinations are just intermediate or end stages for a continuous spectrum of coordination polyhedra that transform into one another. The measure of distortion will depend on the ideal polyhedron we select as representative for a given situation.

The problem of definition for polyhedral distortion can be split into two components: (*a*) regularity of coordination of the central atom (range and scatter of interatomic distances and subtended angles) and (*b*) regularity of the ligand distribution in the polyhedron (coordination sphere).

In the previous contribution (Balić Žunić & Makovicky, 1996) we defined a universal procedure to evaluate the (*a*) and (*b*) components of polyhedral distortion in a scheme dependent on the definition of CN, but not on polyhedral shape. The procedure is based on least-squares fitting of a circumscribed sphere to the polyhedron. It consists of finding a centroid of the polyhedron, calculating the distance of the central atom from the centroid and obtaining a sphericity measure for the polyhedron. The sphericity of the coordination polyhedron has been defined as $(1-\sigma_r/r)$, where r is the radius of the circumscribed sphere and σ_r is the standard deviation of the distances from the centroid to the ligands.

In the present contribution we propose an extension of this scheme in order to express the departure of a polyhedron from its ideal shape. The measure of this departure is a single parameter which can be compared with those of other polyhedra in the same structure (even if they differ in CN) or in a structure family, or over a range of structure types. The proposed measure of distortion concerns the (*b*) component of polyhedral distortion, *i.e.* the regularity of distribution of the ligand atoms irrespective of the position of the central atom in the polyhedron.

2. Calculation procedures

2.1. *Principles*

For every polyhedron type with a given number and topology of faces a polyhedron with the maximum possible volume can be regarded as the ideal one.

Evidently, all platonic polyhedra are ideal or maximum-volume polyhedra for their types. The ratio of the volume of the circumscribed sphere (V_s) to that of the polyhedron (V_p) attains a characteristic value for each ideal/regular polyhedron. It will change with any distortion of the polyhedron from the ideal shape. It will increase with this distortion as long as the centroid–ligand distances and the number and topology of polyhedral faces are preserved. Comparison of the sphere/polyhedron volume ratios (V_s/V_p) for the real and ideal cases (using the sphere volume V_s derived from the real polyhedron) is a suitable global measure of polyhedral distortion of type (*b*).

In those cases when polyhedral deformation breaks up *n*-sided ($n \geq 4$) faces into new sets of triangular faces, this ratio can decrease. The latter cases should therefore be treated as deformed versions of polyhedra with higher numbers of faces. Polyhedra limited by triangular faces (tetrahedra, octahedra, ...) do not experience this kind of distortion. The V_s/V_p ratio can also decrease when the selected ideal polyhedron does not quite correspond to the observed situation as, for example, the capped trigonal coordination prisms in the lillianite homologues described below. The former decrease will be accompanied by increased sphericity of the polyhedron (Balić Žunić & Makovicky, 1996), the latter decrease may be paralleled by a decrease in sphericity.

The first stages of the procedure, circumscription of a sphere to the standard coordination polyhedron by least-squares fitting to all (predefined) ligands, determination of its centre, radius and its standard deviation, have been described by Balić Žunić & Makovicky (1996). Polyhedral volumes can be calculated by dividing the polyhedron into general tetrahedra and summing up their volumes (Balić Žunić & Vicković, 1996).

The sphere/polyhedron volume ratios for the real and the corresponding ideal polyhedron can be compared by means of suitable graphs (Figs. 1–3) or by defining a distortion percentage (υ) as a volume discrepancy between a coordination polyhedron and the corresponding ideal one.

If V_i denotes the volume of the ideal polyhedron and V_r that of the real polyhedron with the same circumscribed sphere radius, the volume discrepancy can be calculated as

$$\upsilon\ (\%) = [(V_s/V_r) - (V_s/V_i)]/(V_s/V_r) \times 100.$$

This expression can be simplified to

$$\upsilon\ (\%) = (V_i - V_r)/V_i \times 100.$$

The volume discrepancy can be used as a quantitative measure of polyhedral distortion (or of the departure from the chosen model).

2.2. *Selected ideal sphere/polyhedron volume ratios*

The volume ratios V_s(circumscribed sphere)/V_p(polyhedron) for regular polyhedra in Table 1 are based on geometric data by Netz & Rast (1986). *r* denotes the centre-to-vertex distance for a regular/ideal polyhedron; *a* is its edge length. The circumscribed sphere shares the radius *r* with the polyhedron. Similar ratios for other ideal coordination polyhedra are derived in the following paragraphs and summarized in Table 2.

Two distinct limiting coordinations CN = 5 are important for the crystal chemistry of Cu with organic ligands; they are interconnected by a spectrum of transitional fivefold coordinations. For these cases, *a* denotes the edge of the base and *l* the inclined edge of the coordination pyramid. The first limiting coordination is a square pyramid with five equal bonds *r* and a Cu atom in the square base (a half-octahedron) (Table 2). The volume of this coordination polyhedron increases when the distance of the vertex from the base increases, drawing the Cu atom into the volume of the pyramid. It reaches a maximum when the height of the pyramid $h = r + \delta$ is equal to $(4/3)r$ (Table 2). The other limiting coordination CN = 5 is a trigonal bipyramid with all centrum-to-ligand distances equal to *r* (Table 2).

A trigonal coordination prism, without or with additional ligands above its rectangular faces ('one- to three-capped prism') is an important coordination polyhedron in inorganic compounds and alloys. Four distinct 'ideal' cases will be examined:

(i) An Archimedean trigonal prism with all nine edge lengths equal to *a* (Table 2). When this prism is capped on 1–3 rectangular faces, with the centre-to-additional ligand (vertex) distance equal to *r*,

$$V_a^{n\text{-capped}} = V_a + (4/7)nr^3(1 - 1/7^{1/2}).$$

$V_s/V_a^{n\text{-capped}}$ is equal to 3.1557, 2.4892 and 2.0551 for n = 1, 2 and 3.

(ii) A trigonal prism with a maximum volume for a given centre-to-vertex distance *r* (Table 2). When this prism is capped with the same caps as the prism of type (i) (the prism centre-to-cap vertex distance is *r*), its volume is

$$V_{\max}^{n\text{-capped}} = V_{\max} + [2(2)^{1/2}/3(3)^{1/2}]nr^3(1 - 1/6^{1/2}),$$

where n = 1–3. For these n values, $V_s/V_{\max}^{n\text{-capped}}$ is equal to 3.1683, 2.5476 and 2.1303 for n = 1, 2 and 3, respectively. These capped cases have total volumes smaller than the following case in which the maximum global volume is calculated for the prism including its *n* caps.

(iii) Parameters for the capped prism with the maximum global volume can be obtained from the general formula for the volume of an *n*-capped trigonal prism with *h* and *r* decoupled. In this case the length *a* of the edge of the prism base is

$$[3r^2 - (3/4)h^2]^{1/2}$$

Table 1. *Geometric characteristics of regular polyhedra (V_p) with a circumscribed sphere (V_s)*

Regular polyhedron	CN	Edge length a	Polyhedral volume	V_s/V_p
Tetrahedron	4	$4r/6^{1/2}$	$8r^3/9(3)^{1/2}$	$9\pi/2(3)^{1/2} = 2.5981\pi = 8.1621$
Octahedron	6	$r(2)^{1/2}$	$(4/3)r^3$	$\pi = 3.1416$
Cube	8	$2r/3^{1/2}$	$8(3)^{1/2}r^3/9$	$(3^{1/2}/2)\pi = 0.8660\pi = 2.7206$
Icosahedron	12	$4r/[2(5+5^{1/2})]^{1/2} = 1.05146r$	$2.5362r^3$	$0.5257\pi = 1.6516$

Note: The centre-to-vertex distance r is the radius of the sphere.

and the global volume is

$$V = [3(3)^{1/2}/4](hr^2 - h^3/4) + (nh)/3^{1/2}[r(r^2 - h^2/4)^{1/2} - r^2/2 + h^2/8]$$
$$= (h/3^{1/2})\{[(9-2n)/4](r^2 - h^2/4) + nr(r^2 - h^2/4)^{1/2}\}.$$

Numerical evaluation of this equation shows that the maximum global volume of the n-capped trigonal prism occurs at: (*a*) $h = 1.2459r$ for a monocapped prism ($V_s/V_p = 3.1424$); (*b*) $h = 1.3129r$ for a bicapped prism ($V_s/V_p = 2.4891$); (*c*) $h = 1.3625r$ for a tricapped prism ($V_s/V_p = 2.0496$). For all these cases, the volume changes which take place with the changing h/r ratio are minor in the broad h/r regions about the value yielding the maximum volumes for capped prisms. Therefore, the incentives to achieve the above-quoted ideal h/r ratios are weak. The calculated V_s/V_p ratios are fairly close to those for an n-capped trigonal prism with all prism edges equal (*i.e.* $a = h$), the above case (i), for which $h = 1.3093r$.

(iv) A monocapped trigonal prism with the 'central' atom in the centre of the square face, which also is a base for the single cap. In order to distinguish it from the above cases with a centrally situated cation, it will be termed 'a split octahedron' (Edenharter, 1976). In this case, r is the distance from this atom to all prism and cap vertices; $a = r^{1/2}$ is the prism height and also the length of all cap edges. The free horizontal edges a' of the prism have length equal to r. Comparing the data in Table 2 with those for the preceding cases we can see that the 'split octahedron' has a larger relative polyhedral volume than the family of monocapped trigonal prisms, cases (i)–(iii). This configuration is approximated in the accommodation of active lone electron pairs in the structure.

An alternative sevenfold coordination has the shape of a pentagonal bipyramid with the centre-to-vertex distance r, for which the 'base cross section' has the area $S = 2.3776r^2$ (Table 2).

Data for a regular coordination cube (CN = 8) are in Table 1. The polyhedron volume for a square antiprism (CN = 8) with the horizontal edges a and height h is

$$V = [(2+2^{1/2})/3]a^2h = \{[4+2(2)^{1/2}]/3\}a^2(r^2 - a^2/2)^{1/2}.$$

Two limiting situations for this coordination, the Archimedean antiprism with all edge lengths equal to a and the antiprism with maximum volume, are specified in Table 2.

For atoms with CN = 12 four ideal polyhedra, the *cuboctahedron, anticuboctahedron, icosahedron* and maximum volume *hexagonal prism*, occur in competition. Parameters for the cuboctahedron and icosahedron are in Table 1; those for anticuboctahedron (in the h.c.p. arrays) coincide with the former. A hexagonal prism with a given centre-to-vertex distance r, horizontal edges a and prism height h has volume equal to

$$\frac{3}{2}(3)^{1/2}(hr^2 - h^3/4).$$

This volume becomes the tabulated maximum (Table 2) for $h = 2(3)^{1/2}r/3$. The results for an irregular 12-fold coordination may be compared with the three ideal V_s/V_p values and conclusions on its proximity to (or deformation of) any of these drawn.

3. Applications

The proposed global measure of polyhedral distortion can be used to quantify:

(*a*) Deviations of coordination polyhedra from ideal shapes.

(*b*) Degree and types (branches) of isotypy/homeotypy (Lima-de-Faria *et al.*, 1990) by comparison of distortion characteristics of analogous polyhedra in the structures of one isotypic/homeotypic family.

(*c*) Quantification of departures from a structural archetype (Makovicky, 1989).

(*d*) Measure of distortion of complicated structures (*e.g.* tectosilicates) from their aristotype (Megaw, 1973).

(*e*) Configurational driving mechanisms for phase transformations.

Examples of these applications follow; each of them illustrates several of the above points.

4. Examples

Sartorite homologues $Pb_{4N-8-2x}As_{8+x}Ag_xS_{4N+4}$ are a series of Pb–As sulfides with zigzag walls composed of columns of tricapped trigonal coordination prisms of Pb. The walls alternate with variously thick slabs composed of monocapped 'lying trigonal prisms' ('split octahedra') of As and Pb; these slabs are based on an SnS archetype.

The closely related Tl–As–Sb sulfides contain columns of alternating Tl and Sb prisms rather than tricapped Pb prisms and Sb partly or fully replaces As in the 'SnS-like' slabs. At an advanced stage of the latter substitution these structures move from the SnS to the PbS archetype in the slabs. In this work we compared the coordination polyhedra of baumhauerite $Pb_6As_8S_{18}$ (Engel & Nowacki, 1969), a typical member of the sartorite series, with those of pierrotite $Tl(Sb,As)_5S_8$ (Engel *et al.*, 1983) and parapierrotite $TlSb_5S_8$ (Engel, 1980).

Tricapped Pb prisms in the structure of the typical sartorite homologue follow closely the ideal V_s/V_p ratio for the trigonal prisms of type (i); $\upsilon = 0.0$–1.6% (Fig. 1). Those of Tl in pierrotite and parapierrotite are more deformed (υ = 3.0–6.9%). Sb in these prisms exhibits moderate polyhedral distortion in the Tl–Sb–As sulfide pierrotite (υ = 5.2–6.9%), but it displays a very pronounced polyhedral distortion in the Tl–Sb member parapierrotite (υ = 26.8–27.5%). This is connected with a highly asymmetric position of Sb in the flattened polyhedron; also the disposition of Tl and Sb prisms changes between pierrotite and parapierrotite.

'Lying monocapped prisms' of As, and of associated Pb and Sb in baumhauerite and pierrotite follow the maximum-volume ratio in Fig. 1. Those of Sb in the Tl–Sb sulfide parapierrotite preserve the polyhedral volume of prisms in the As–Sb members, whereas the volume of a sphere circumscribed around them increases by ~36%; the resulting deformation measure υ for CN = 7 is about 22%. It is a *measure of change from a SnS-like to a PbS-like configuration*, which takes place with the full occupation of SnS-like layers by Sb.

Lillianite homologues (for most cations $M^{2+}_{N-1}M^{3+}_{2}S_{N+2}$) consist of variously wide PbS-like slabs with CN = 6, cut out and twinned on $(311)_{PbS}$, creating intervening walls of bicapped trigonal coordination prisms (CN = 8) on their boundaries. Both types of coordination polyhedra can be occupied by a spectrum of cations. Fig. 2 shows the generally low degree of polyhedral distortion in this series. The bicapped trigonal prisms follow the maximum-volume V_s/V_p ratio [case (iii)] and the same is true for the octahedra in the slabs. In lillianite homologues with Pb in trigonal prisms, the V_s/V_p ratio decreases slightly in comparison to the maximum-volume prism ($\upsilon = -3.3\%$), because these prisms deviate from the ideal definition – the capping ligands are much more distant than those forming the trigonal prism. In the structure of the lillianite homologue $TlSb_3S_5$ (Gostojić *et al.*, 1982), the combined distortions of the bicapped trigonal coordination prisms of Tl result in $\upsilon = 0.2\%$. For both the Pb prisms and the Tl prisms the sphericity values (Balić Žunić & Makovicky, 1996) are reduced substantially, to 94%. The coordination octahedra of Sb are very distorted in $TlSb_3S_5$ (υ = 12.8–19.8%). A decrease in the octahedron volume with increasing distortion is caused by a sideways movement of the sixth ligand rather than its shift along the axis of the elongated octahedron.

The degree of polyhedral distortion in the sartorite and lillianite families is a direct function of lone-electron-pair activity of cations in the SnS-like or PbS-like slabs. The former with their 'split-octahedral' coordinations (CN = 7) are fit to accommodate the very active (*i.e.* volume demanding) lone electron pairs of As; the latter, with little deformed octahedral coordinations (CN = 6) exist because of the low electron-pair activity of Bi. Introduction of a cation with intermediate lone-electron-pair activity into either of these two structure types leads to coordination states intermediate between

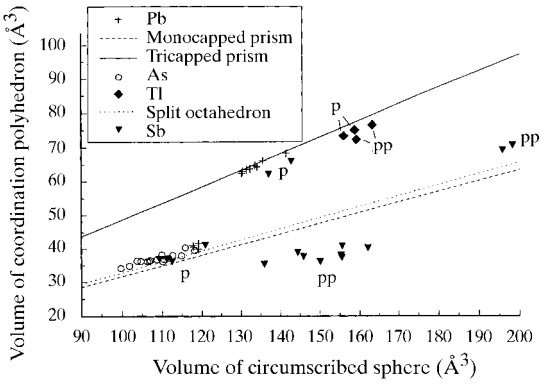

Fig. 1. Ratio of the volume of a least-squares circumscribed sphere to the volume of a coordination polyhedron for cations in the sulfides of the Pb–As sartorite homologous series and related Tl–As–Sb sulfides. Ratios for ideal polyhedra are indicated by correlation lines. p: pierrotite, pp: parapierrotite. Structure references are given in the text.

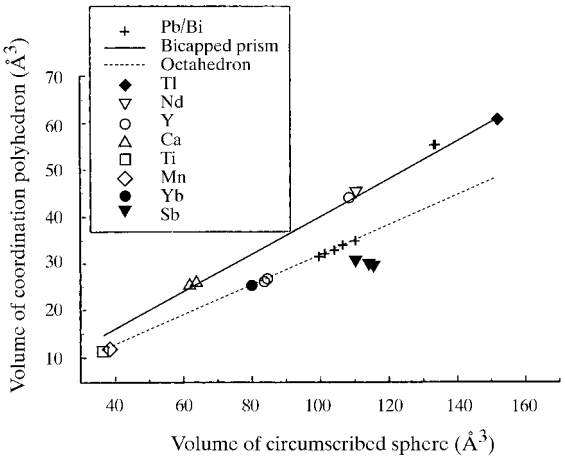

Fig. 2. The V_s/V_p ratios for cations in typical undistorted and distorted lillianite homologues (unit-cell twinned cation-filled c.c.p. arrays). Correlation lines show ratios for ideal polyhedra. References for the structures: lillianite (Takagi & Takeuchi, 1972), heyrovskyite (Takeuchi & Takagi, 1974), $TlSb_3S_5$ (Gostojić *et al.*, 1982), $CaMn_2O_4$ (Couffon *et al.*, 1964; Lepicard & Protas, 1966), $CaTi_2O_4$ (Bertaut & Blum, 1956), $NdYbS_3$ (Carré & Laruelle, 1974), Y_5S_7 (Adolphe, 1965).

Table 2. *Geometric characteristics of additional ideal coordination polyhedra*

Ideal polyhedron	CN	Edge length a	Height h	Inclined edge length l	Polyhedral volume	V_s/V_p
Archimedean square pyramid	5	$r(2)^{1/2}$	r	$r(2)^{1/2}$	$(2/3)r^3$	$2\pi = 6.2832$
Square pyramid with maximum volume	5	$(4/3)r$	$(4/3)r$	$[2(3)^{1/2}/3]r$	$(64/81)r^3$	$1.6875\pi = 5.3014$
Trigonal bipyramid	5	$r(3)^{1/2}$	$(2)r$	$r(2)^{1/2}$	$(3^{1/2}/2)r^3$	$1.5396\pi = 4.8368$
Archimedean trigonal prism	6	$(12/7)^{1/2}r$	$(12/7)^{1/2}r$	—	$[18/7(7)^{1/2}]r^3$	$[14(7)^{1/2}/27]\pi = 4.3099$
Trigonal prism with maximum volume	6	$r(2)^{1/2}$	$(2/3^{1/2})r$	—	r^3	$(4/3)\pi = 4.1888$
'Split octahedron'	7	$a = r(2)^{1/2}$; $a' = r$	$r(2)^{1/2}$	$r(2)^{1/2}$	$\{[4 + 3(2)^{1/2}]/6\}r^3$	3.0491
Pentagonal bipyramid	7	$2r\sin 36^\circ = 1.1756r$	$(2)r$	$= a$	$1.5851r^3$	2.6427
Archimedean square antiprism	8	$[2(2)^{1/2}/(4 + 2^{1/2})^{1/2}]r$	$2r/[2(2)^{1/2} + 1]^{1/2}$	$[2(2)^{1/2}/(4 + 2^{1/2})^{1/2}]r$	$1.7189r^3$	2.4369
Square antiprism with maximum volume	8	$(2/3^{1/2})r$	$(2/3^{1/2})r$	$[2(4 - 2^{1/2})^{1/2}/6^{1/2}]r$	$\{[16 + 8(2)^{1/2}]/9(3)^{1/2}\}r^3 = 1.7522r^3$	$\{3(3)^{1/2}/[4 + 2(2)^{1/2}]\}\pi = 2.3906$
Hexagonal prism with maximum volume	12	$(2/3)^{1/2}r$	$[2(3)^{1/2}/3]r$	—	$2r^3$	$(2/3)\pi = 2.0944$
Cuboctahedron	12	r	$r(2)^{1/2}$	r	$[5(2)^{1/2}/3]r$	$[4/5(2)^{1/2}]\pi = 1.7772$

Note: The centre-to-vertex distance r is also the radius of the circumscribed sphere.

those above and the observed polyhedral/structural distortions.

The coordination polyhedra of cavity cations in *feldspars* $M_x^+M_{1-x}^{2+}Si_{2+x}Al_{2-x}O_8$ show V_s/V_p ratios smaller than the predicted V_s/V_p ratio in the idealized model of the feldspar structure derived by Hyde & Andersson (1989). The relation between polyhedral volumes and the circumscribed sphere volumes departs from a linear one and converges with the increasing radius of the large cation towards the value for the idealized model for both CN = 9 and CN = 10 (Fig. 3).

The coordination polyhedron of a large cation filling the aluminosilicate framework of feldspars is hard to relate to any regular polyhedron. For CN = 9 the Na–Ca feldspars show the worst values of sphericity, augmented V_s/V_p ratios and largest eccentricity (Fig. 4), because of the deformations connected with small cation size. All these characteristics are best for intermediate cation sizes (Sr–Ba), suggesting the most regular distribution of anions around the large cation site. In monoclinic feldspars for CN = 9 the coordination polyhedron contains two four-cornered faces, in triclinic feldspars only triangular faces. Still, this difference does not suffice to lower the V_s/V_p ratio of the triclinic Na–Ca feldspars below that of adjacent monoclinic feldspars of Sr and Ba.

The rise in sphericity slows down for the largest cations; their eccentricity rises moderately, whereas their V_s/V_p ratio rises appreciably for K and Rb. Hyde & Andersson's (1989) ideal feldspar does not follow these trends (Fig. 4). The three polymorphs of $KAlSi_3O_8$ display a progressively better V_s/V_p ratio (*i.e.* a decrease in polyhedral distortion) with decreasing formation temperature. For the entire feldspar series, the altered Si/Al ratios do not appear to influence the configuration values substantially (Fig. 4).

When compared to a tricapped trigonal coordination prism with the maximum global volume, the distortion

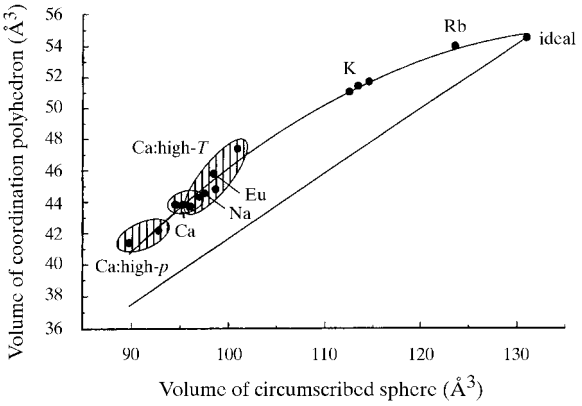

Fig. 3. V_s and V_p values for coordination polyhedra CN = 10 of cavity cations in feldspars together with the value for an idealized feldspar structure (Hyde & Andersson, 1989). The straight line is the V_s/V_p ratio calculated from this idealized structure. References for Figs. 3 and 4 are: K-feldspars: sanidine (Scambos *et al.*, 1987), orthoclase (Colville & Ribbe, 1968) and microcline (Griffen & Johnson, 1984); Rb-feldspar (Gasperin, 1971), albite $NaAlSi_3O_8$ (Armbruster *et al.*, 1990), anorthite $Ca_2Al_2Si_2O_8$ (Wainwright & Starkey, 1971), high-T anorthite (Foit & Peacor, 1973), high-p anorthite (Angel, 1988), Eu-feldspar (Kimata, 1988), Sr-feldspar (Grundy & Ito, 1974), hyalophane (Ba-K feldspar) (Viswanathan & Kielhorn, 1983) and celsian $Ba_2Al_2Si_2O_8$ (Newnham & Megaw, 1960).

Table 3. *Configurational characteristics for coordination polyhedra in Fe–Mg cummingtonite*

Polyhedron	CN	Space group	V_r (Å^3) ΔV_r (high to low)	V_s/V_r	υ (%)	Centroid-to-cation distance (Å)	x_{Fe}
*M*1	6	*C*2/*m*	12.125	3.190†	1.52	0.03	0.20
		$P2_1/m$	12.035	3.191	1.55	0.03	0.20
			−0.74%				
*M*2	6	*C*2/*m*	11.995	3.174	1.03	0.06	0.09
		$P2_1/m$	11.918	3.176	1.10	−‡	0.09
			−0.64%				
*M*3	6	*C*2/*m*	11.853	3.212	2.20	0.00	0.17
		$P2_1/m$	11.837	3.207	2.05	0.02	0.16
			−0.13%				
*M*4	6	*C*2/*m*	11.610	4.367	28.06	0.37	0.91
		$P2_1/m$	11.532	4.391	28.45	0.39	0.91
			−0.67%				
	7	*C*2/*m*	18.061	3.072§	0.74	0.56	0.91
		$P2_1/m$	17.595	3.050	0.04	0.48	0.91
			−2.58%¶				
*T*1	4	*C*2/*m*	2.178	8.162††	0.00	0.01	—
*T*1*A*	4	$P2_1/m$	2.176	8.169	0.08	0.01	—
*T*1*B*	4	$P2_1/m$	2.185	8.166	0.04	0.02	—
			average Δ = 0.23%				
*T*2	4	*C*2/*m*	2.187	8.203	0.50	0.04	—
*T*2*A*	4	$P2_1/m$	2.181	8.226	0.78	0.03	—
*T*2*B*	4	$P2_1/m$	2.210	8.208	0.56	0.03	—
			average Δ = 0.39%				

† For an ideal octahedron this ratio is equal to 3.142. ‡ Cannot be calculated due to a misprint in the original publication (Yang & Smyth, 1996). § For an ideal 'split octahedron' (CN = 7) this ratio is equal to 3.049 (υ is related to this value). ¶ ΔV_r for CN = 8 is −1.14% (change from 24.512 to 24.232 Å^3; V_s/V_r alters from 2.495 to 2.517). †† For an ideal tetrahedron this ratio is equal to 8.162.

percentage for CN = 9 in all feldspars lies between 18.6 and 22.0%. Alternatively, when we understand the ninefold coordination in feldspars as *a deformed cube with an additional ligand* positioned above the midpoint of the cube edge, we can compare its volume with that of a regular cube supplemented with such a ninth ligand positioned at the same centroid–ligand distance as the other eight ligands. The V_s/V_p ratio for an ideal 'cube + 1' configuration is $[3(3)^{1/2}/(4+6^{1/2})]\pi = 2.53108$. The deviations of V_s/V_p from this value are fairly negligible for feldspars (below 2% and mostly close to 0). Only for the idealized model and the Rb-feldspar does this deviation rise to 4 and 3.6%, respectively. These results suggest that this unusual coordination polyhedron is fully justified for the description of feldspar structures.

The departure of the V_s/V_p trend from linearity shows that the effect of incorporating a large cation into the aluminosilicate framework is that of straining it towards its limit of deformability on both ends of the cation-size spectrum and that it is possible to measure the strain of the framework in silicates by the V_s/V_r relations and related configuration characteristics.

Polyhedral differences between the *C*2/*m* and $P2_1/m$ forms of *ferromagnesian cummingtonite* $(Fe,Mg)_7Si_8O_{22}(OH)_2$ (Yang & Smyth, 1996) are summarized in Table 2. These structures consist of *M* and *T* coordination polyhedra occupied, respectively, by (Fe,Mg) and Si. When the *M*4 site is defined as six-coordinated, it is a very distorted octahedron; comparison of seven-coor-

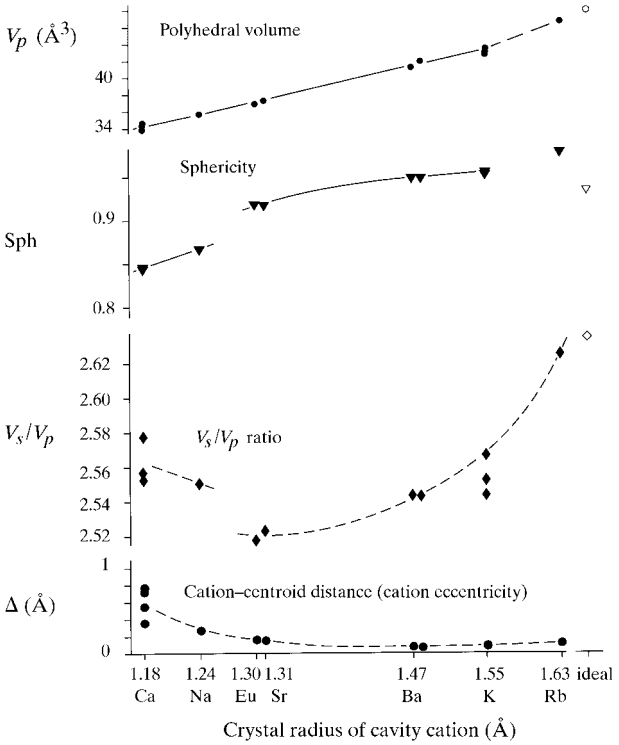

Fig. 4. Polyhedral volume V_p, V_s/V_p ratio, sphericity and cation eccentricity for CN = 9 for the cavity cations in feldspars of Ca, Na, Eu, Sr, Ba, K and Rb at ambient conditions, plotted against the cation crystal radius (Shannon, 1976). For references see Fig. 3.

dinated $M4$ with a 'split octahedron' gives for $M4$ about the same space-filling efficiency as this ideal polyhedron and only a small distortion percentage.

Comparison of the configurational characteristics for the $C2/m$ and $P2_1/m$ phases shows that the driving force of phase transformation on cooling is the volume reduction (−2.6%) and regularization of the $M4$ polyhedron on the CN = 7 level without a marked shift of the cation position inside this polyhedron (Table 3). The CN = 6 and CN = 8 'levels' of the $M4$ polyhedron, as well as the $M1$–$M3$ octahedra and the T tetrahedra, change little on transformation, their reduction being in line with the overall unit-cell volume reduction of 0.62% between 295 and 140 K.

Analysis of approximately 25 ABX_3 compounds isopointal (Lima-de-Faria *et al.*, 1990) with *ilmenite* (Bergerhoff, 1996) reveals that for all non-controversial cases, which primarily are double oxides, V_s of the octahedra for each of the smaller cations are rather constant. The only significant crystal-chemical subdivision of this series results from plotting the distortion percentages for the A and B coordination octahedra against the central atom–centroid distances in them (Fig. 5).

Two well defined groups of isotypes can be discerned:

(i) *Ilmenite isotypes*, in which Ti is the small B cation with an appreciably eccentric position in its octahedron. The B octahedron is less distorted than those of larger, less eccentric A cations.

(ii) *$ZnGeO_3$ isotypes*, in which Si^{4+}, Ge^{4+}, Sn^{4+} or As^{5+} play the role of the small B cation, which is in the structure combined with a fairly large A cation. Both the larger distortion and the larger eccentricity are here reserved for the octahedra of the larger A cations (Fig. 5).

$ZnTiO_3$ illustrates a case of questionable structure determination.

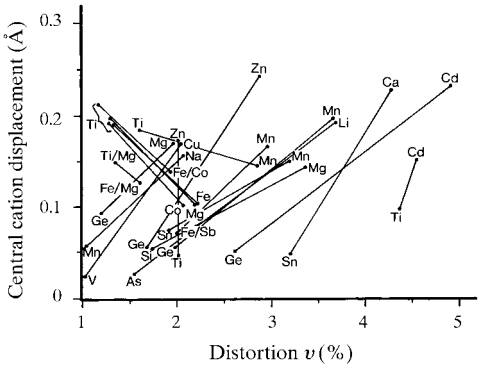

Fig. 5. Central cation displacement (*i.e.* cation eccentricity) *versus* polyhedral distortion for the coordination octahedra in double oxides isopointal with ilmenite. Data from the Inorganic Crystal Structure Database (Bergerhoff, 1996). Solid lines interconnect cations belonging to the same structure. Ilmenite isotypes and $ZnGeO_3$ isotypes can be discerned according to the resulting line slope.

These selected examples show that the global measure of polyhedral distortion proposed in this paper is a suitable tool for the configurational analysis of a number of structural families. Both the families based on simple idealized coordination polyhedra and those with complex coordinations can be analysed, especially when the global measure of distortion is combined with other distortion characteristics.

The authors profitted from discussions of these concepts with a number of crystallographic colleagues, especially with Dr G. Bergerhoff (Karlsruhe), as well as from the comments of two anonymous reviewers. The professional assistance of Mrs Maybritt Handest and Mrs Britta Munch is gratefully acknowledged.

References

Adolphe, C. (1965). *Ann. Chim.* **10**, 271–297.
Angel, R. J. (1988). *Am. Mineral.* **73**, 1114–1119.
Armbruster, T., Buergi, H. B., Kunz, M., Gnos, E., Broennimann, S. & Lienert, C. (1990). *Am. Mineral.* **75**, 135–140.
Balić Žunić, T. & Makovicky, E. (1996). *Acta Cryst.* B**52**, 78–81.
Balić Žunić, T. & Vicković, I. (1996). *J. Appl. Cryst.* **29**, 305–306.
Bergerhoff, G. (1996). Written communication.
Bertaut, E. F. & Blum, P. (1956). *Acta Cryst.* **9**, 121–126.
Carré, D. & Laruelle, P. (1974). *Acta Cryst.* B**30**, 952–954.
Carter, F. L. (1978). *Acta Cryst.* B**34**, 2962–2966.
Colville, A. A. & Ribbe, P. H. (1968). *Am. Mineral.* **53**, 25–37.
Couffon, M.-M., Rocher, G. & Protas, J. (1964). *C.R. Acad. Sci.* **258**, 1847–1849.
Edenharter, A. (1976). *Schweiz. Mineral. Petrogr. Mitt.* **56**, 195–217.
Engel, P. (1980). *Z. Kristallogr.* **151**, 203–216.
Engel, P., Gostojić, M. & Nowacki, W. (1983). *Z. Kristallogr.* **165**, 209–215.
Engel, P. & Nowacki, W. (1969). *Z. Kristallogr.* **129**, 178–202.
Foit, F. F. & Peacor, D. R. (1973). *Am. Mineral.* **58**, 665–675.
Gasperin, M. (1971). *Acta Cryst.* B**27**, 854–855.
Gostojić, M., Nowacki, W. & Engel, P. (1982). *Z. Kristallogr.* **159**, 217–224.
Griffen, G. T. & Johnson, B. T. (1984). *Am. Mineral.* **69**, 1072–1077.
Grundy, H. D. & Ito, J. (1974). *Am. Mineral.* **59**, 1319–1326.
Hyde, B. G. & Andersson, S. (1989). *Inorganic Crystal Structures*, pp. 399–403. New York: John Wiley & Sons.
Kimata, M. (1988). *Mineral. Mag.* **52**, 257–265.
Klebe, G. & Weber, F. (1994). *Acta Cryst.* B**50**, 50–59.
Lepicard, G. & Protas, J. (1966). *Bull. Soc. Fr. Mineral. Cristallogr.* **89**, 318–324.
Lima-de-Faria, J., Hellner, E., Liebau, F., Makovicky, E. & Parthé, E. (1990). *Acta Cryst.* A**46**, 1–11.
Lueken, H., Elsenhans, U. & Stamm, U. (1987). *Acta Cryst.* A**43**, 187–194.
Makovicky, E. (1989). *Neues Jahrb. Mineral. Abh.* **160**, 269–297.
Megaw, H. D. (1973). *Crystal Structures: A Working Approach.* Philadelphia: W. B. Saunders Co.
Netz, H. & Rast, J. (1986). *Formeln der Matematik/Netz*, 6th ed., p. 607. München–Wien: Carl Hauser Verlag.

Newnham, R. E. & Megaw, H. D. (1960). *Acta Cryst.* **13**, 303–312.
Robinson, K., Gibbs, G. V. & Ribbe, P. H. (1971). *Science*, **172**, 567–570.
Scambos, T. A., Smyth, J. R. & McCormick, T. C. (1987). *Am. Mineral.* **72**, 973–978.
Shannon, R. D. (1976). *Acta Cryst.* A**32**, 751–767.
Takagi, J. & Takeuchi, Y. (1972). *Acta Cryst.* B**28**, 649–651.
Takeuchi, Y. & Takagi, J. (1974). *Proc. Jpn Acad.* **50**, 76–79.
Toraya, H. (1981). *Z. Kristallogr.* **157**, 173–190.
Viswanathan, K. & Kielhorn, H. M. (1983). *Am. Mineral.* **68**, 122–124.
Wainwright, J. E. & Starkey, J. (1971). *Z. Kristallogr.* **133**, 75–84.
Weiss, Z., Rieder, M., Chmielová, M. & Krajíček, J. (1985). *Am. Mineral.* **70**, 747–757.
Yang, H. & Smyth, J. R. (1996). *Am. Mineral.* **81**, 363–368.